

63L.0 EXPERIMENTALLY VALIDATING PHASE FIELD MODELING OF DILUTE Al-Cu ALLOYS WITH OXIDE PARTICLES PRESENT

Spencer Hunt (Mines)

Faculty: Amy Clarke, Kester Clarke, Mohsen Asle-Zaeem (Mines)

Industrial Mentor: TBD

This project initiated in Fall 2021 and is supported by the NSF. The research performed during this project will serve as the basis for a MS thesis program for Spencer Hunt.

63L.1 Project Overview and Industrial Relevance

As liquid metal is poured into a mold during casting, it may be exposed to atmosphere to produce oxides. Oxide layer formation is especially prevalent in aluminum alloys. Due to the liquid metal turbulence typically seen during casting, a thin oxide layer on the surface of Al can potentially fold on itself, resulting in an unbonded oxide-oxide interface known as a bi-film (**Figure 63L.1**). The bi-film can become entrapped within the melt, impacting casting quality. The unbonded surface of the bi-film can act as a pre-existing crack, which can propagate with further processing, such as extrusion, which imparts stresses. The mechanical properties have yet to be fully understood, but there also lies a knowledge gap in understanding the effect of oxide bi-films on solidification structure evolution, specifically regarding the nucleation of phases and the formation of dendritic structures and defects.

Multi-billion atom molecular dynamic (MD) and quantitative phase-field modeling (PF) simulations are often implemented to understand the atomic interactions during solidification within a melt. In order to accurately simulate atomic interactions, 2NN-MEAM+QEq interatomic potentials were developed for various Al binary alloys by Asle Zaeem et al. (Mines). Since then, MD and PF simulations have been completed on dilute Al-Cu alloys with Cu compositions ranging from 1-11 at% [63L.1]. These initial simulations have been completed without implementing oxides. Current work is being done to include oxides to better understand their role on solidification. A. Clarke et al. (Mines) has previously combined in-situ x-ray imaging of solidification with PF simulations to better understand solidification mechanisms in dilute Al-Cu alloys [63L.2]. We will use novel processing and characterization capabilities available at Mines, including state-of-the-art electron microscopy and a custom x-ray radiography cabinet capable of in-situ solidification experiments with special platforms, to study the interaction of oxides in solidifying microstructures of select binary Al-Cu alloys. Results obtained from these experiments will be used to inform MD and PF modeling. A conceptual schematic for the project is shown in **Figure 63L.2**.

63L.2 Previous Work – Literature Review

Defects may be oxide related and take on a bi-film morphology. As oxides are introduced in the melt through convection and other disturbances in the melt, they can have a range of effects on the solidifying microstructure. Oxide bi-films can become “unfurled” and become effective convection barriers, preventing both thermal and mechanical perturbations, allowing for grains to grow to abnormally large sizes [63L.4]. On the other hand, if many small bi-films are present, grain refinement can occur as these small bi-films fragment advancing dendrites while they are being circulated around the melt through convection effects. Oxides are known to be ineffective nucleation sites for primary phases, while they are effective nucleation sites for secondary phases. Because of this, a region effectively surrounded by oxides can see large amounts of undercooling, as there are no nucleation sites for the primary phase. This can lead to an extremely fine secondary dendrite arm spacing when sufficient undercooling is achieved [63L.4]. While this may be an extreme occurrence, it goes to show how oxides can affect solidification in

an important way. To date, many findings regarding oxides have been mostly conjecture, with no direct observations being made. This has led to a lack of basic understanding of bi-film evolution and interactions with solidifying material. Using the advancements in x-ray radiography and computational modeling, experimentally validated computational modeling will help to bring a new understanding on the important role oxides play on solidifying microstructures.

63L.3 Recent Progress

63L.3.1 Introducing Oxides in the Material – Accumulative Roll Bonding (ARB)

An obstacle for this work is introducing oxides in a manner that is reproducible, controllable, and simulates physical castings. Accumulative roll bonding (ARB) consists of stacking two sheets of materials and roll bonding them with approximately 50% reduction [63L.5]. This results in a single sheet, nominally the same thickness as a single original sheet with twice the length. The as-rolled material is then sectioned in half, degreased, and stacked, thereby constituting one roll bonding cycle. Prior to rolling, the sheets will be inevitably exposed to the atmosphere and form a thin oxide layer (<10 μm). When the material is bonded, the oxide layers are entrapped in the material, forming a long discontinuous oxide layer at the now bonded interface plane where the two plates meet. The amount of oxide desired can be controlled by controlling surface oxidation between the bonding passes and the number of roll bonding passes performed, with each pass increasing interface layers following the relationship shown in Equation 63L.1, where L_i and L_f indicates the number of layers before and after the pass, respectively.

$$L_f = 2(L_i) + 1 \quad \text{Equation 63L.1}$$

Once these oxides are entrapped in the material, they can be used to simulate oxides entrapped in a typical casting. Trials of performing the ARB process on Al-7Cu (at. %) plate have been completed with some edge cracking. Many factors affect the success of the ARB process, but the two factors discussed for this work are the temperature of the material being rolled and the mitigation of edge cracking. Successful bonding was achieved by heating the material to 300 °C and then immediately rolling, effectively increasing the ductility and promoting bonding [63L.6] [63L.7]. Despite the elevated temperature, edge cracking was still prevalent (**Figure 63L.3**). In the future, edge cracking will be avoided by using constraints to prevent movement/misalignment of the plates as they are being rolled, either by using wire to bind the strips together, or using the guides on the rolling mill itself. To avoid lateral spreading, it has been found that machining a sacrificial frame of a more ductile material prevents lateral spread cracking of the roll bonding sample, which will be pursued in the future for this project [63L.6] [63L.7].

63L.3.2 Melt and Solidify Material - Laser Track Melting

With oxides introduced by ARB, laser track melting will be pursued to melt and solidify the material, due to its ease of access, speed, and ability to control the solidification velocity through the speed of the scan. Initial obstacles have involved finding the correct processing parameters, such as scan speed, power, and focal offset distance (FOD). Ideally, the parameters chosen would produce a melt pool that penetrates 75-100% of the thickness of roll bonded sample. Less than this could produce a melt pool that doesn't encapsulate the oxide layers produced by ARB. Initial scans were performed, keeping the travel speed and FOD constant, 100 in/min and 0, respectively, and varying the power between 600-1200 W. Initial track melts at 1000 W on 2 mm thick material led to promising initial results with good penetration. Replicating these parameters, laser track melts were performed on materials with 0, 1, and 2 ARB cycles. Upon documenting the microstructure of the melt pools, it was found that some were reaching full penetration, but also contained iron (**Figures 63L.4 and 63L.5**) likely originating from the steel base plate during the track melting. Surface reflectivity varied between the as-received material and ARBed

63L.2

material, altering the effective energy input from a given laser welding condition. Future work will address the changes in laser parameters or surface preparation required to achieve equivalent welding conditions on as-received and ARBed material.

63L.3.3 Imaging Using the X-Ray Cabinet

Mines has recent acquired a custom high-powered x-ray cabinet in the laboratory which can obtain 2D radiography and 3D computed tomography. Dr. Amy Clarke has previous experience using x-ray imaging to compare in-situ observations to model predictions. This work was done at Los Alamos National Laboratory (LANL) and at the Advanced Photon Source (APS) at Argonne National Laboratory using a furnace set up that is shown in **Figure 63L.6**. This involves using a boron nitride crucible to hold the sample and a steel rod connected to two induction coils that are independently heated to melt the sample. This furnace was installed directly in the beam line for in-situ synchrotron X-ray imaging. Both components have a central hole, allowing x-rays to interact with the solidifying sample. A thin surface oxide layer prevents the metal from spilling during the experiment [63L.2]. For this work, similar experiments may be conducted in the x-ray cabinet at Mines.

63L.4 Plans for Next Reporting Period

- Roll material up to 8 ARB cycles to create various dispersions of included oxides in an aluminum matrix.
- Using laser track melting to produce representative melt pools for characterization to inform modeling.
- Within the melt pools, document oxide interactions with solidification structures.
- Pursue building a furnace set-up for in-situ solidification radiography in the x-ray cabinet at Mines.

63L.5 References

- [63L.1] G. Azizi, M. Asle Zaeem, S. Kavousi, Interactive Effects of Interfacial Energy Anisotropy and Solute Transport on Solidification Patterns of Al-Cu Alloys, unpublished
- [63L.2] D. Tourret, J.C.E. Mertens, E. Lieberman, S.D Imhoff, J.W. Gibbs, K. Henderson, K. Fezzaa, A. L. Deriy, T. Sun, R.A. Lebensohn, B.M. Patterson, A.J. Clarke, From Solidification Processing to Microstructure to Mechanical Properties: A Multi-scale X-ray Study of an Al-Cu Alloy Sample. Metallurgical and Materials Transaction A, vol. 48, (2017) 5529–5546
- [63L.3] Griffiths, W.D., Raiszadeh, R., Hydrogen, porosity and oxide film defects in liquid Al. Journal of Material Science 44, (2009) 3402–3407
- [63L.4] J. Campbell, et al.. An overview of the effects of bifilms on the structure and properties of cast alloys. Metallurgical and Materials Transactions, vol. 37B, (2006) 863
- [63L.5] B. McBride, Accumulative Roll Bonding of AA 5083 Toward Low Temperature Superplasticity (Brady McBride’s Graduate Thesis), publication pending, (2022) 41-48
- [65L.6] B. McBride, K. D. Clarke, A. J. Clarke, Mitigation of Edge Cracking During Accumulative Roll Bonding (ARB) of Aluminum Strips, Journal of Manufacturing Processes vol. 55 (2020) 236-239
- [63L.7] Y. Saito, H. Utsunomiya, N. Tsuji, T. Sakai, Novel Ultra-High Straining Process For Bulk Materials - Development of the Accumulative Roll Bonding (ARB) Process, Acta Materialia. 47 (1999) 579–583.

63L.6 Figures and Tables

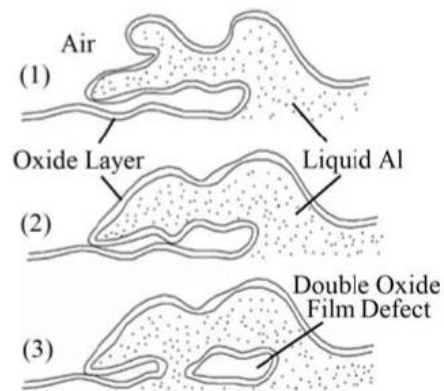


Figure 63L.1: Oxide formation on the surface of a casting transitioning to an oxide bi-film through turbulence in the liquid [63L.3]

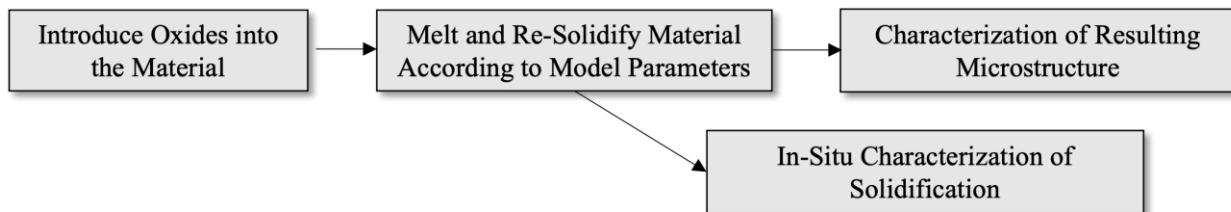


Figure 63L.2: Conceptual schematic for the project describing the general experimental approach and subsequent characterization.

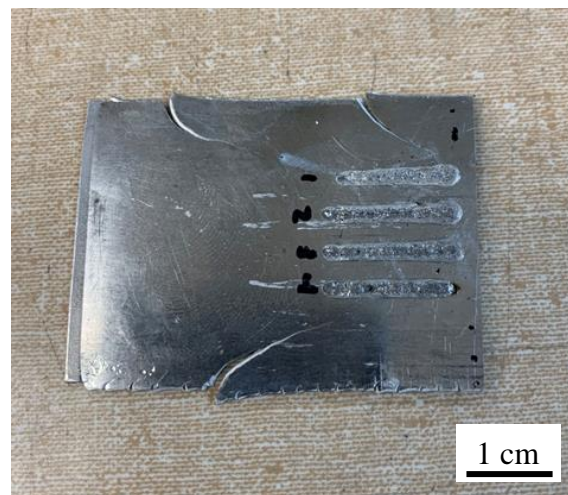


Figure 63L.3: Successfully roll bonded (1 Pass) 1mm thick Al-7Cu (at%) plates, material preheated at 300 °C prior to rolling. Four laser track melts were performed on the roll-bonded material. Width of rolled strip is approximately 50 mm.

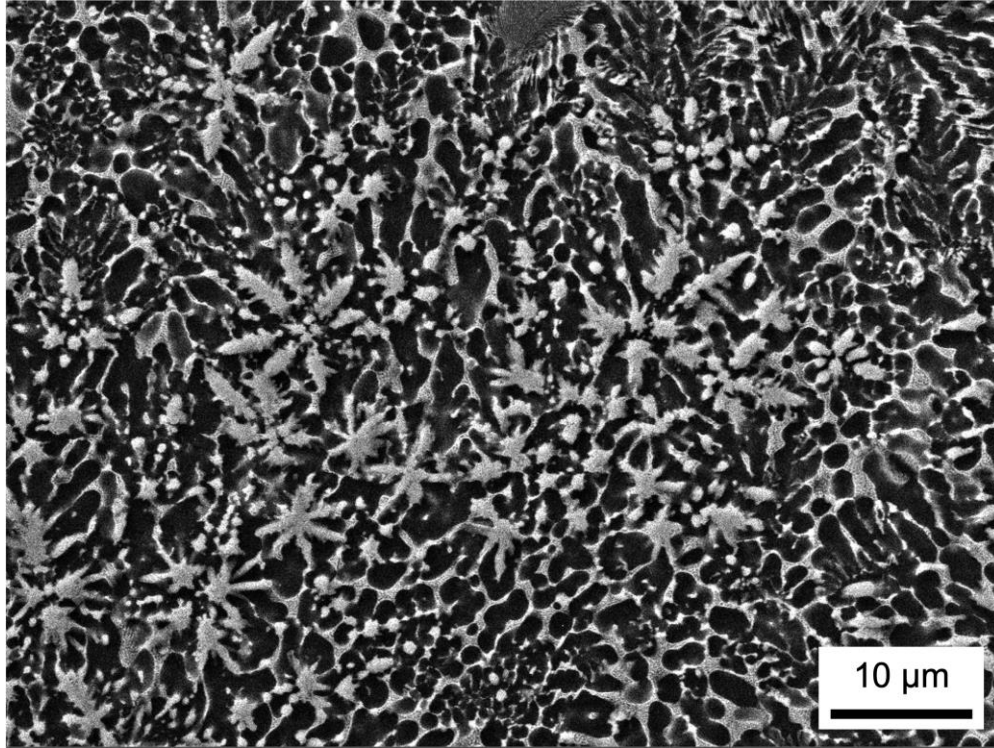


Figure 63L.4: SEM secondary electron image of a melt pool where full penetration was achieved and iron contamination was present, 3.94kx magnification, 6.00mm WD.

63L.6

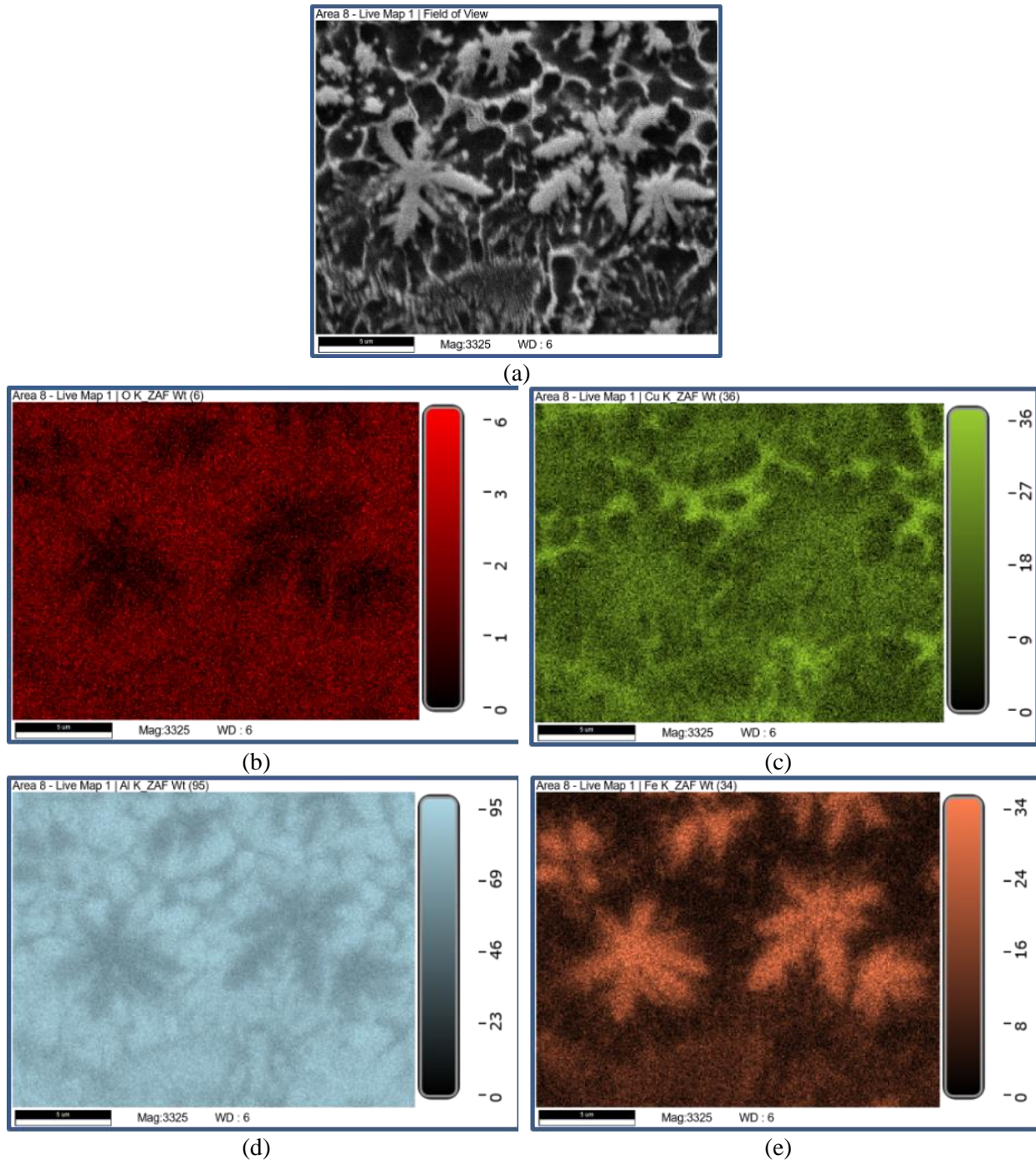


Figure 63L.5: EDS maps and data of 0 ARB layer material dendrites found in the center of the melt pool; a) SE image of the area b) EDS map of oxygen content of the area; c) EDS map of aluminum content of the area; d) EDS map of iron content of the area; e) EDS map of oxygen content of the area.

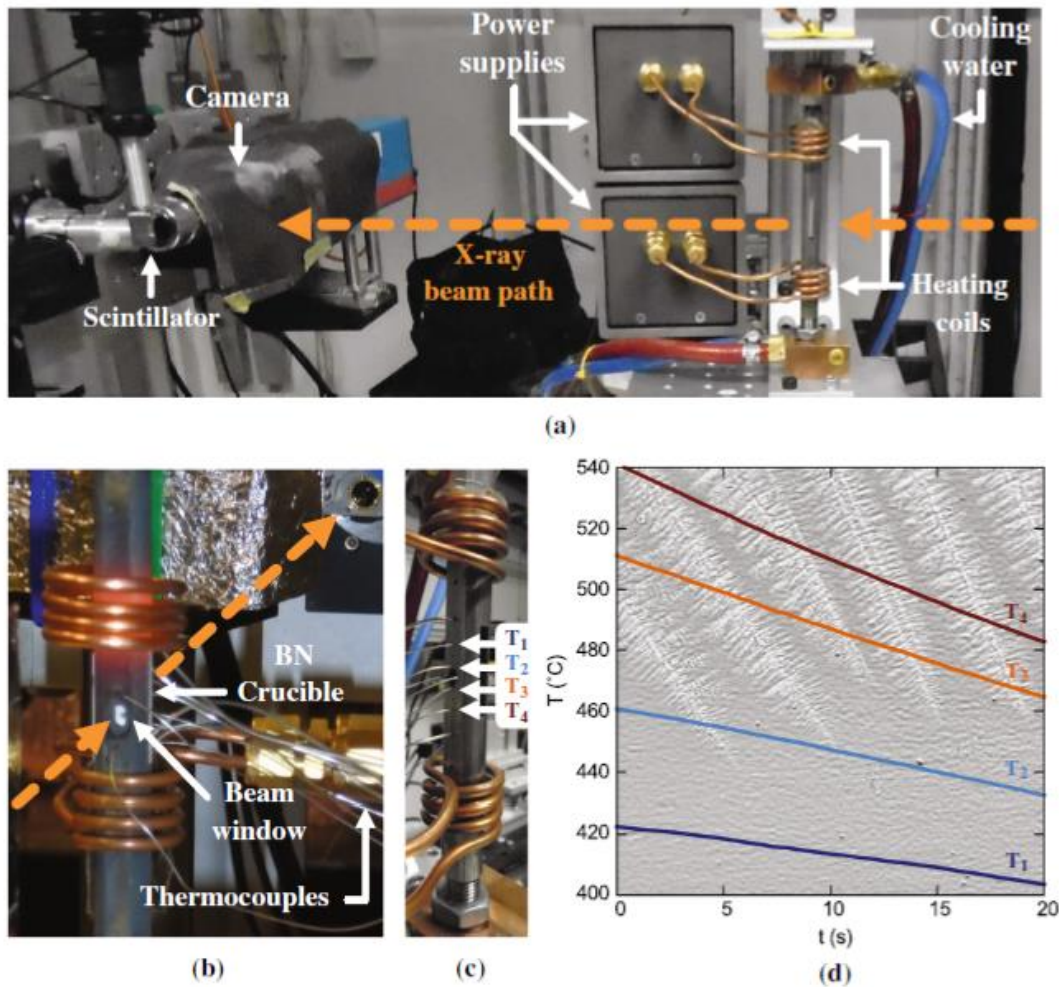


Figure 63L.6: Directional solidification furnace setup installed at Argonne National Laboratory's Advanced Photon Source. (a) shows the induction furnace with an empty steel rod. The heated steel rod in (b) contains a boron nitride (BN) crucible with a partially melted sample. (c) provides a detailed view of the thermocouples, and (d) shows the temperature evolution measured by four of these thermocouples as the dendrite front swipes through the field-of-view for the specific sample discussed throughout the article. Note that, unlike in (b), the solidification of this sample proceeds from the top downward, as in the background image of (d), i.e., with $T_1 < T_2 < T_3 < T_4$. Figure and caption taken from [63L.6].